INFRASTRUKTURA I EKOLOGIA TERENÓW WIEJSKICH
INFRASTRUCTURE AND ECOLOGY OF RURAL AREAS

No IV/2/2017, POLISH ACADEMY OF SCIENCES, Cracow Branch, pp. 1619–1631
Commission of Technical Rural Infrastructure

DOI: http://dx.medra.org/10.14597/infraeco.2017.4.2.122

DETERMINATION OF THE INFLUENCE OF BUILDING MASS ON LANDSLIDE FORMATION USING UNMANNED AERIAL SYSTEMS

Józef Sanecki, Andrzej Klewski, Marek Zygmunt, Grzegorz Stępień
Maritime University in Szczecin

Abstract

Following the torrential rain and floods that occurred between 1997 and 2010, there has been an emergence of new and previously activated processes related to soil and rock landslides in the Polish Carpathians. In light of the damage incurred by landslides, there is a problem with the thorough diagnosis of the nature of phenomena and thus the development of methods to prevent landslides in the future. This article discusses the problem of surveying landslide areas. It highlights the possibility of using photogrammetric methods for digital imaging, as well as determines the dimensions when estimating the mass of buildings within the area of a landslide, with particular emphasis on the use of an unmanned aerial system (UAS). The described method for obtaining processing images involves a non-metric camera mounted on a UAS. The designed projections centre on individual images and elements of angular orientation and the camera interior. This enables the creation and texturing of a triangulated irregular network (TIN) model. The final result in this work is a digital surface model (DSM) and an orthophotomap. It was found that characteristic land types have been occurring in the landslide substrate with key parameters determining their properties. This enabled the determination of a resistance ground border and provided an opportunity to examine whether a building of known mass may be the main cause of a landslide.

Keywords: aero triangulation, UAS, DSM, landslide, geological structure.

INTRODUCTION

Since prehistoric times, landslides have occurred in places of intensive colonization. In one example, landslides features included the flattening of the central part of a slope, which was screened in the upper part by a high afforested escarpment, while the lower part of the slope was overgrown by forest. This was caused by local mountain climate relaxation, which created appropriates sites for colonization (Bajgier-Kowalska 2004-2005). In this case, buildings were initially built of wood, such that their mass would not cause the activation of mass movements. Problems appeared when people began building brick buildings on landslide areas, which could be one of the reasons why numerous old landslides have been reactivated in recent years. The surveying issues concerning landslides result from the unwitting construction of residential buildings and outbuildings on such vulnerable areas.

For the first time in Poland, surface surveying on landslide areas was performed on a large scale during the realization of the Landslide Protection System (SOPO) project (http://geoportal.pgi.gov.pl). By surveying landslides' mass movements, their speed and character were determined. The SOPO coordinators used a direct measurements method, in which the surveying of a network of stabilized points was performed at least three times a year. Table 1 presents the results, together with the given X,Y,Z coordinates. The coordinators carried out their surveying with GPS equipment, as well as used statistics methodology with baseline data (Szafarczyk 2011). The main purpose of the work was determination of the influence of building mass on landslide formation using unmanned aerial systems.

AREA OF RESEARCH

The landslide at the centre of this investigation is located in the west part of Węgierka village in the Rożwienica commune. All of the landslide area has an east slope elevation and lies within Płaskowyż Jawornicki, which is a part of Pogórze Dynowskie. The landslide area occupies exactly 20 ha. The upper and middle parts of the landslide have been inactive from more than 50 years. Landslide activity is determined in the work of Grabowski *et al*. (2008). The area is smooth and has been used agriculturally for many years. The landslide topography looks like a wavy package of rocks and soil, which are visible in the lower active part. Besides residential buildings and outbuildings, there is a school, a chapel with a cemetery, a school's transmission lines and an asphalt road. Activation at the low part of the landslide has caused a lot of damage; for example, the construction of two outbuildings was breached and the road surface was destroyed, while electric masts have shifted (Kurkowski *et al*. 2012).

This damage constitutes the basis for carrying out research in the landslide area in question. In June 2016, a photogrammetric search was conducted with a DJI Phantom 3 Professional UAS. Using the obtained images, a DSM of the lower part of the landslide was created with an eyelet mesh of 0.10 m (Stępień 2016). This in turn accurately defined the shape and dimensions of the buildings on the landslide, as well as their position in relation to other elements of space. This part of the landslide area and the points above sea level were also mapped. In the future, it will be possible to further observe landslide development. Localisation of study area is on Figure 1.

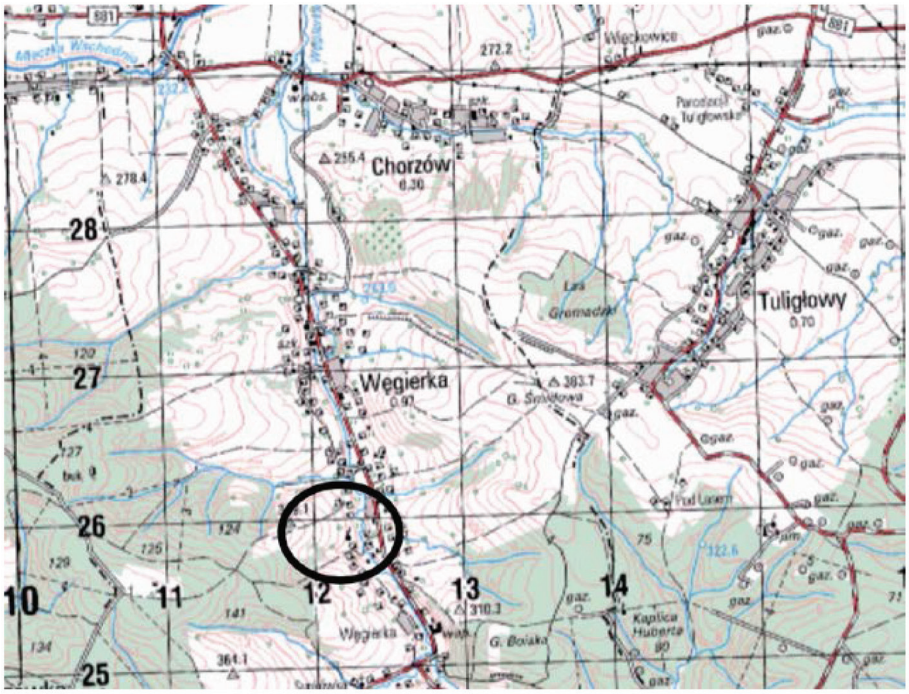

Source: WODGiK Rzeszów

Figure 1. Localisation of study area

GEOLOGY OF THE LANDSLIDE AREA

The landslide lying within the Skolska nappe is located in the outside part of the Carpathians Mountains, which is characterized in the upper section by Cretaceous and Palaeocene formations. Meanwhile, the Inoceramus layers are from the Eocene epoch, the Hieroglyphic layers are from the Oligocene epoch,

and the Menilite and Krosno layers are from the Miocene epoch. The rock formations occur in sandstone-slate facies. The Inoceramus and Hieroglyphic layers are responsible for creating marginal folds (Gucik *et al*. 2003). The angle of collapsed rocks varies along the borders from 20° to 65°, although we can observe layers that lie horizontally or upright (Zabuski *et al.* 1999). The geological composition of the study area is on Figure 2.

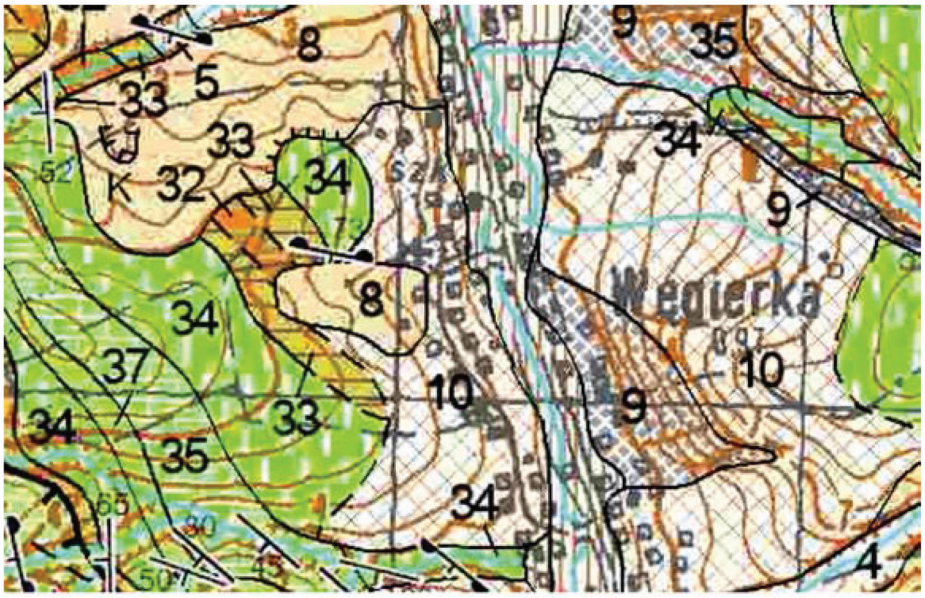

Source: SMGP ark. Rokietnica

Figure 2. The geological composition of the study area

Next to the upper part of the landslide, rock formations are visible within the riverbed scarp of the Węgierka River. There is an overlay of different soils, such as diluvium soils in the form of clay, sandy clay with sandstone and slate inserts, and limestone. There are also loams with slate inserts and sands with gravel. The thickness of the sedimentary cover is about 2.0 – 4.5 m (Piskadło 2010).

The underground waters in this area occur in sandstone layers and slate rocks. The underground water level was drilled at a depth of 2.1 – 2.3 m under the area level.

The geotechnical characteristics of ground substrates were identified via microscopic analysis of ground samples conducted during field research, supported by the analysis of archival materials and the PN-81-B-03020 standard.

We separated out the geotechnical layers as follows:

Layer I contains material that slides and is detached from slopes, such as clay with a hard plastic consistency. This ground is fine-grained and very intumescent with medium cohesiveness. The medium degree of ductility is I_L=0.20 (indicator of consistency I_C=0.80). These soils contain minor inserts of sandstone and slate.

Layer II is created by coarse-grained ground (loose/non-cohesive), which has developed in a similar way to medium sands and grey gravel in a medium concentrated state, or is humid or rehydrated. The medium degree of compaction is I_D=0.40. This ground is non-intumescent and, similar to clays, is found in slides and detached material.

Layer III comprises fine-grained ground (medium cohesiveness), which has developed in the same way as grey sandy clays in a ductility state. The middle indicator of plastic is I_L=0.30 (indicator of consistency I_C=0.70), with some humidity. These clays contain crumbled pieces of sandstone with a predominance of slate. They are found in slides and detached ground from slopes.

Layer IV comprises clays that occur in a hard plastic state, i.e., I_L=0.05, and border with low-lying weathered loamy limestone. The same weathered limestone occurs in the slip space of slides and detached material. This space is located at a depth of 2.5-3.0 m under the area level (Piskadło 2010). Many slate inserts help to create the landslide (Zydroń 2015).

Layer V is caused by defaulting in ground-weathered loamy limestone and includes marl from Węgierka village (Gucik *et al*. 2003) with ground in different granulations. The clays and loams, along with clay sandstone admixtures, result in a hard plastic consistency.

Under this layer is located rocky ground in the form of loamy slate and fine-grained sandstone. In the Inoceramus and Hieroglyphic layers, the durability of these rocks is highly differentiated: Rc=0.4 – 50 Mpa (Piskadło 2010).

Based on ductility degree I_L and compaction degree I_D, the values of other characteristic geotechnical parameters of the ground from the landslide area were calculated. The results are shown in Table 1.

Table 1. The characteristic geotechnical parameters from the landslide area

Number of geo-technical layers	Ground symbol	Depth under the area level	Ground state	Com-paction degree I_D	Ductility degree I_L	Con-sistency indicator IC	Volumetric density P [t×m^{-3}]	Angle of internal friction Φ [°]	Cohesion Cu [kPa]
I	G	Clay (0-0.7 m p.p.t)	tpl	-	0.20	0.80	2.15	14.8	16.9
II	Ps	Sand (0.7-1.4 m p.p.t)	szg	0.40	-	-	1.85	32.4	0.00
	Ż	Gravel (2-2.1 m p.p.t)					1.90	37.7	
III	Gp	Clay with sand (1.4-2.1 m p.p.t)	pl	-	0.30	0.70	2.10	13.2	13.3
IV	I	Loam (2.1-2.5 m p.p.t)	tpl	-	0.05	0.95	2.00	17.2	25.6
V	KWg	Weathered loamy limestone (2.5-4.5 m p.p.t)	pzw	-	0.00	1.00	2.25	18.0	30.0

pl – ductility ground [I_C=0.50-0.75] or [I_L=0.25-0.50]
tpl – hard ductility ground [I_C=0.75-1.00] or [I_L=0.00-0.25]
szg – the medium compaction ground [I_D=0.33-0.67]
pzw – half compact ground [I_C>1.00] or [I_L < 0.00]

MATERIAL AND METHODS

In order to elaborate the DSM and orthophotomap, a photogrammetric flight mission was made above the landslide area. For this purpose, the Phantom 3 Professional UAS, manufactured by DJI, was used. The flight mission was made at a medium relative height of 70 m. The UAS carried a camera with constant parameters (3.61 mm) and a physical pixel size in matrix form (1.56 μm) allowed for a ground resolution element of 0.027 m to be obtained. The flight mission was made on a sunny day with light wind (gusts below 5 m/s). The longitudinal and side overlap was about 80%. The camera predominantly faced the Sun (mostly in vertical photos). In the process, 262 photos were taken, which

were subjected to further rectification. The elaboration process of the DSM and orthophotomap was made using the Agisoft PhotoScan computer program. This elaboration included the following stages:

1. Loading photos and project creation
2. Aerotriangulation with autocorellation of images
3. Generation and classification of dense point clouds
4. TIN model creation
5. Texturing of the TIN model
6. Tiled model creation
7. DSM generation
8. Orthophotomap generation
9. DSM and digital orthophotomap export
10. Report generation

After loading the photos, a project was created and reference layout EPSG 2179 was set up (coordinate system PUWG 2000, zone 8). The next step was to carry out aerotriangulation with self-calibration in the course of aligning the photos. During this process, the perspective centres of individual photos were designated, corrected and aligned. Elements of exterior and interior camera orientation were also designed. In this way, aerotriangulation was completed. The analytical relationships between elements of the exterior and designated space coordinates for every point can be described according to the following equation (Stępień *et al*., 2016):

$$\begin{bmatrix} X \\ Y \\ Z \end{bmatrix} = \begin{bmatrix} X_0 \\ Y_0 \\ Z_0 \end{bmatrix} + \lambda \begin{bmatrix} 1 & 0 & 0 \\ 0 & cos\omega & sin\omega \\ 0 & -sin\omega & cos\omega \end{bmatrix} \begin{bmatrix} cos\varphi & 0 & -sin\varphi \\ 0 & 1 & 0 \\ -sin\varphi & 0 & cos\varphi \end{bmatrix} \begin{bmatrix} cos\kappa & -sin\kappa & 0 \\ sin\kappa & cos\kappa & 0 \\ 0 & 0 & 1 \end{bmatrix} \begin{bmatrix} x \\ y \\ z \end{bmatrix} \quad (1)$$

- where:
  - ω – rotation around the x axis
  - φ – rotation around the y axis
  - κ – rotation around the z axis,
  - X, Y, Z – coordinates in the secondary system (aerial)
  - x, y, z – coordinates in the primary system (sensor)
  - X_0, Y_0, Z_0 – translation vector (shift systems)
  - λ – coefficient change of scale (during perspective transformation)

As a result of aerotriangulation, it was possible to create dense point clouds for this classification in order to construct and texture the TIN model.

After creating dense point clouds, a tiled model was formulated in order to generate the final elaborations. The first step was to create the DSM with an eyelet mesh of 0.10 m, followed by the orthophotomap. The DSM was ex-

ported to the XYZ format, while the digital orthophotomap was exported to the GeoToff format.

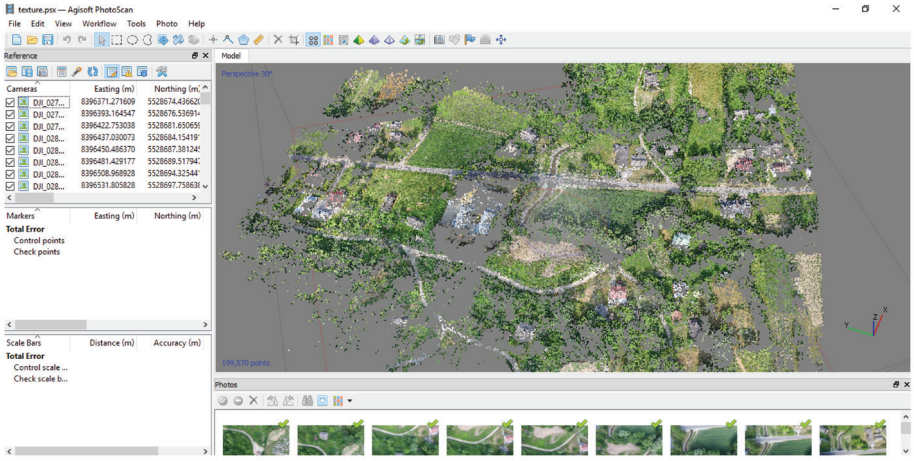

Source: Authors' own study

Figure 3. Aerotriangulation with autocorellation of images (matched points on the images)

Source: Authors' own study

Figure 4. Digital orthophotomap of the landslide: pixel size (ground sampling distance) = 0.027 m

The final stage of the work involved regenerating the raport. During the processing stage, average error points were identified for location X, Y on the orthophotomap at the 100 pixels level. In effect, the location of the points of absolute accuracy were at the level of about 1.1 m. Regarding height (DSM), the Z coordinate was obtained as follows: 165 pixels and 1.5 m absolute accuracy. Relative accuracy was obtained within limits of 3 pixels (0.08 m) for the X, Y coordinates and 5 pixels (0.11 m) for the Z coordinate (height – DSM).

DISCUSSION

Based on the DSM for the low landslide part, the construction calculations for the executive project for the cardiology clinic in Bielsk Podlaski (Zabagło, 2014) and the cadastral map of area, the estimated medium building mass on field no. 761/1 was 85 tons. Localisation of building is on Figure 5.

Source: www.geoportal.gov.pl

Figure 5. Localisation of building

According to the calculated value of the mass, there is a pressure force caused by building on the landslide. This value is 834 kN. The calculated val-

ues of the ground's geotechnical parameters allow us to determine the pressure force for the ground's border resistance Q_f, which counteracts the pressure force of building Q_r. To calculate this, we used the following equation from the PN-81-B-03020 standard:

$$Q_f=BL[(1+0.3B/L)N_c c_u^{(r)} i_c+(1+1.5B/L)N_D r_D^{(r)} g D_{min} i_D+(1-0.25B/L)N_B r_B^{(r)} g L i_B] \quad (2)$$

where:
Q_{fNL} – vertical component of the computational ground's border resistance (kN)
e_B, e_L – centre of burden, accordingly in the horizontal direction in relation to the B width and the L length at the foundation foot (m)
D_{min} – depth of foundation, measured from the lowest aerial level (m)
N_c, N_D, N_B – coefficients of load capacity
$F_u^{(r)}$ – computational value of the angle of internal friction on the ground directly under the foundation level (°)
$c_u^{(r)}$ – computational value of the cohesive ground directly under the foundation level (kPa)
$r_D^{(r)}$ – computational average volume density of the ground above the foundation level
$r_B^{(r)}$ – computational average volume density of the ground under the foundation level to a depth equal to B
g – acceleration of gravity, $m \cdot s^{-2}$ ($g=9.81\ m \cdot s^{-2}$)
i_C, i_D, i_B – coefficients' influence on the slope's encumbered force.

RESULTS

As a result of the calculations made, the following extreme values of the border resistance of the ground's force for individual kinds of ground were determined:

- Clay, weathered loamy limestone and loam with the minimum ductility degree value (I_L=0.00) and a maximum angle of internal friction value ($F_u^{(r)}$=18°) – 495.00 kN
- Clay, weathered loamy limestone and loam with the maximum ductility degree value (I_L=1.00) and the minimum angle of internal friction value ($F_u^{(r)}$=2.1°) – 14.44 kN
- Sand, gravel with the maximum compaction degree value (I_D=1,00) and the minimum angle of internal friction value ($F_u^{(r)}$=42.1° for gravel; 36.1° for sands) – 4,399.50 kN
- Sand, gravel with the minimum compaction degree value (I_D=0.00) and the maximum angle of internal friction value ($F_u^{(r)}$=34.8° for gravel; 29.9° for sands) – 881.43 kN

The value of Q_f changes according to the angle of internal friction $F_u^{(r)}$ on the ground upon which building foundations are placed. Cohesive soils (clays,

loams) have low values for the angle of internal friction (only a few degrees). While cohesionless ground (sands, gravel) has higher values (tens of degrees), it is clearly visible that foundations placed upon cohesive ground (clays, loams) can cause buildings to subside. That said, the landslide is only able to move if all the ground layers are detached from the substrate and postponed along the slip surface. Only this kind of surface can cause saturation of the ground by water, as it cannot occur on impermeable rocks (slate, marls). In turn, the building can accelerate the movement of the landslide, as the lower part of the landslide is active. This causes considerable damage to buildings and the road infrastructure. Furthermore, the mass of a single building, along with violent heavy rain and the presence of a landslide slope, can indirectly cause this part of the landslide to be activated.

CONCLUSIONS

1. The DSM of the landslide with an eyelet mesh of 0.10 m can define the localization and dimensions of a building with great precision. This supports research into the influence of buildings on mass movements.
2. The research shows that single building cannot induce a landslide. However, if it is located on cohesive ground, this can increase the probability of mass movements.
3. In the area of a landslide, the building mass can indirectly activate the lower part of the landslide.
4. As a result of placing foundations on cohesive ground (clays, loams), subsidence can occur and buildings can tilt.
5. The value of ground border resistance Q_f can change within a wide range, depending on the angle of internal friction $F_u^{(r)}$, ductility degree I_L and compaction degree I_D of the ground.
6. A digital orthophotomap at a ground resolution of 0.027 m, created as a result of orthophotos taken by a UAS, allows for more detailed observation of location objects in a landslide area and the space relations occurring between them.
7. In order to achieve high levels accuracy in non-metric camera imaging, aerotriangulation should be performed with additional parameters. Accurately designed photogrammetric control is necessary.
8. The location of points with high relative and absolute accuracy allows for the broad utilization of close-range photogrammetry methods, especially involving a UAS, to document damage in landslides areas.
9. Photogrammetric elaborations with transverse and oblong orthophotos can cover 80% of landslides areas, enabling the production of reliable measurements and information in support of SOPO activities.

10. The measurement system, which was designed and used during the landslide survey, proved to be practical and useful.

REFERENCES

Bajgier-Kowalska M. (2004-2005). *Rola gospodarczej działalności człowieka w powstawaniu i odmładzaniu osuwisk w Karpatach fliszowych*. Kraków. Folia Geographica Series Geographica-Physica, XXXV-XXXVI:11-30.

Grabowski D., Marciniec P., Mrozek T., Nescieruk P., Rączkowski W., Wójcik A., Zimnal Z. (2008). *Instrukcja opracowania Mapy osuwisk i terenów zagrożonych ruchami masowymi w skali 1:10000*. Warszawa: CAG Państwowy Instytut Geologiczny-Państwowy Instytut Badawczy.

Gucik S., Kucharska M., Piotrowska K. (2003). *Szczegółowa mapa geologiczna Polski w skali 1:50 000 ark. Rokietnica (1007) wraz z objaśnieniami.* Warszawa: CAG Państwowy Instytut Geologiczny-Państwowy Instytut Badawczy.

Kurczyński Z. (2014). *Fotogrametria*. Warszawa: PWN.

Kurkowski S., Zygmunt M. (2012). *Objaśnienia do Mapy Osuwisk i Terenów Zagrożonych Ruchami Masowymi w skali 1:10000 dla gminy Roźwienica.* Warszawa: CAG Państwowy Instytut Geologiczny-Państwowy Instytut Badawczy.

Piskadło R. (2010). *Ekspertyza Geotechniczna dla ustalenia geotechnicznych warunków posadowienia drogi gminnej i budynku mieszkalnego nr 151 po naruszeniu stateczności zbocza osuwiskami w miejscowości Rogi, gmina – Miejsce Piastowe*. Zespół Usług Geologiczno-Technicznych "HGS-EKO". Krosno, ul. Czajkowskiego 55.

Stępień G., Sanecki J., Klewski A., Beczkowski K. (2016). *Wyznaczanie granic użytków rolnych wykorzystaniem bezzałogowych systemów latających*. Infrastruktura i ekologia terenów wiejskich, Nr III/2: 1011-1024.

Szafarczyk A. (2011). *Geodezyjne metody monitoringu osuwisk*. Infrastruktura i Ekologia Terenów Wiejskich, 2/2011: 293-300.

Zabagło Z. (2014). *Założenia i obciążenia przyjęte do obliczeń konstrukcji, zastosowane schematy konstrukcyjne oraz podstawowe wyniki obliczeń dla Projektu wykonawczego Kliniki Kardiologii Inwazyjnej przy ul. Kleszczelowskiej 1 w Bielsku Podlaskim*. Atelier ZETTA. Białystok, ul. Suraska 2/11.

Zabuski L., Thiel K., Bober L. (1999). *Osuwiska we fliszu Karpat polskich. Geologia, modelowanie, obliczenia stateczności.* Gdańsk: Wyd. IBW PAN.

Zydroń T. (2015). *Właściwości geotechniczne łupków pstrych z okolic Szymbarku koło Gorlic*. Acta. Sci. Pol. Formatko Circumiectus 14(2): 231-241.

Polska Norma PN-81-B-03020. *Grunty budowlane. Posadowienie bezpośrednie budowli. Obliczenia statyczne
i projektowanie*. UKD 624.131.5:624.15. Grupa katalogowa 0702.

Wojewódzki Ośrodek Dokumentacji Geodezyjnej i Kartograficznej w Rzeszowie. Mapa w skali 1:50 000

http://geoportal.pgi.gov.pl [access: 01.11.2016]

http://www.geoportal.gov.pl

Corresponding author: Marek Zygmunt, MSc
Józef Sanecki, Professor
Andrzej Klewski, Associate Professor
Grzegorz Stępień, PhD

Institute of Geoinformatics,
Żołnierska 46, 71-250 Szczecin
Tel.: +48 506 567 596
Email: marek.zygmunt@op.pl

Received: 03.04.2017
Accepted: 20.11.2017